Transactions of the Korean Nuclear Society Autumn Meeting
Jeju, Korea, October 21-22, 2010

An image quality approach for optimizing ^{124}I PET imaging on Siemens Inveon PET Scanner

A Ram Yu [a,b], Jin Su Kim [a*], Gwang Il An [a], Sang Keun Woo [a], Jong Guk Kim [a], Ji Ae Park [a], Gi Jeong Cheon [a], Byeong Il Kim [a], Chang Woon Choi [a], Sang Moo Lim [a], Hee Joung Kim [b], Kyeong Min Kim [a]
[a]*Molecular Imaging Research Center, Korea Institute Radiological and Medical Science, Seoul, Korea*
[b]*Department of Radiological Science, College of Health Science, Yonsei University, Wonju 220-710, Korea*
[*]*Corresponding author: kjs@kirams.re.kr*

1. Introduction

^{124}I has a long half life of 4.2 days that is suitable for imaging over several days during the biological uptake and washout of radioiodine. However ^{124}I has a low positron branching ratio (23%). High-energy γ- photons (602 keV to 1,326 keV) are emitted in cascade with the positrons. These cascade γ- photons degrade the image quality [1,2]. To find optimal parameter, image quality of the Inveon ^{124}I PET scanner with various energy window settings was measured based on the NEMA NU4-standars and compared with those of ^{18}F PET.

2. Methods and Results

2.1 Detector Characteristics

The Inveon PET scanner is intended for the imaging of small animals that is high sensitivity, high resolution preclinical PET scanner.

The detector consists of 64 detector blocks arranged in 4 full rings with LSO (lutetium oxyorthosilicate) based on crystal ring diameter of 16.1 cm and axial FOV of 12.7 cm. Total 25,600 LSO crystals are composing 80 detector rings so each ring has 320 crystals. Detector block consists of 20x 20 arrays and1.51 x1.51 x10 mm^3 individual crystal arranged with a pitch of 1.59 mm to allow the high packing fraction (92%). LSO crystals coupled to a position sensitive photomultiplier tube via a light guide and highly reflective material is interposed between the crystals [3,4].

2.2 NEMA NU4 Image Quality Phantom

The NEMA NU4 image quality phantom (length 50 mm, diameter 30 mm, and volume 20.7 ml) is consisted of three parts in cylindrical. Space of the center is uniform region (length 15 mm, diameter 30 mm) and this part means actual signal to noise of imaging equipment. The upper part of the uniform region is cold region that have two empty spaces (length 15 mm, inner diameter 8 mm, and outer diameter 10 mm). One space fills air and the other space fills nonradioactive water. Although both cylinders are nonradioactive, scattered photons, nonzero positron range, random or other effects may cause the reconstructed images display activity in these compartments. Bottom of the cylinder (length 20 mm, diameter 30 mm) has five fillable rods with diameters of 1, 2, 3, 4, and 5 mm and center of each rod is 7 mm from the cylinder axis. This part serves recovery coefficient (RC) [5,6].

The image quality phantom was positioned on the center of scanner FOV and energy window settings were 250 ~ 550, 250 ~ 650, 250 ~ 750, 350 ~ 550, 350 ~ 650, and 350 ~ 750 keV and timing window was set to 3.432 nsec.

2.3 Assessment of the Uniformity

The volume of interest (VOI) of cylindrical volume (length 10 mm, diameter 22.5 mm) was drawn for the measurement of the uniformity.

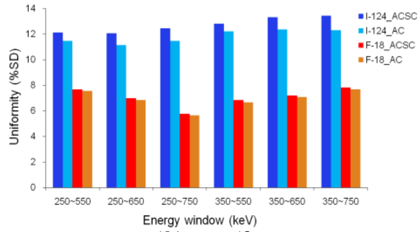

Fig. 1. The uniformity of ^{124}I and ^{18}F acquired in various energy windows.

The uniformity of the ^{124}I and ^{18}F were shown in Figure 1. Overall, the uniformities of ^{124}I were two times of those of ^{18}F. The lowest uniformity was 12.06% (^{124}I) in 250~650 keV and 5.77% (^{18}F) in 250~750 keV. When scatter correction was applied, %SD was slightly increased.

2.4 Assessment of the Recovery Coefficient

The circular ROIs were drawn on each rod. The recovery coefficient (RC) defined as the ratio between the measured maximum values in the rods and the mean value in the uniform area. The SD of the pixel values measured along each line profile was used to determine the mean and SD of the RC for each rod size. %SD of the RC was calculated by the following equation.

$$\%SD_{RC} = 100 \times \sqrt{\left(\frac{SD_{lineprofile}}{Mean_{lineprofile}}\right)^2 + \left(\frac{SD_{uniformregion}}{Mean_{uniformregion}}\right)^2}$$

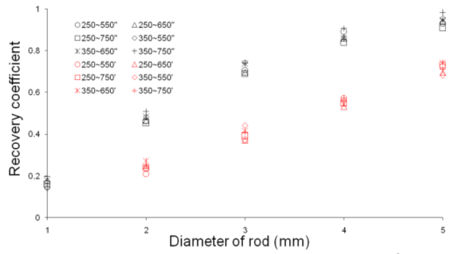

Fig. 2. Recovery coefficient of ^{124}I and ^{18}F.

The highest value of RC was in 250~750 keV for ^{124}I and 350~750 keV for ^{18}F.

%SD of RC was increased in wider energy window and this tendency was clear for ^{124}I.

2.5 Assessment of the Spillover Ratio

Two cylindrical VOIs (length 7.5mm, diameter 4mm) in the air and water filled compartments were drawn. The spillover ratio (SOR) defined as the ratio of mean value in each cold cylinder and the mean value in the uniform area. The %SD of SOR was also calculated in the same equation used for the RC.

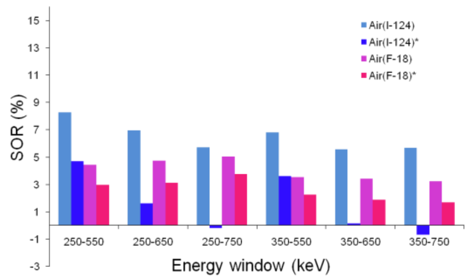

(a)

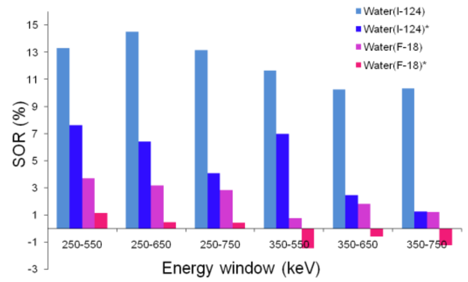

(b)

Fig. 3. SOR of cold cylinder (air (a), water (b)). Point marker (*) means when scatter correction was applied.

SORs in the water and air compartments were shown in Figure 3 for the 2 radionuclides with and without scatter correction. ^{18}F clearly showed lower SOR than ^{124}I in water and air compartments in all energy windows. In water, the different of SOR among 2 sources was larger than in air. The SORs in water were considerably higher for ^{124}I than for ^{18}F.

3. Conclusions

In terms of image quality parameters, the performance of ^{124}I PET was lower than ^{18}F PET. These differences were due to characteristics of radionuclide. The abundance of high energy γ-photons and large positron ranges were affected image quality.

Considering the image quality, optimized energy window was 250~750 keV for ^{124}I.

REFERENCES

[1] R. A. Gregory, C. A. Hooker, M. Partridge, and G. D. Flux, Optimization and assessment of quantitative ^{124} I imaging on a Philips Gemini dual GS PET/CT system, European Journal of Nuclear Medicine and Molecular Imaging, Vol.36, No. 7, pp. 1037-1048, 2009.

[2] H. Herzog, L. Tellmann, S. Qaim, S. Spellerberg, A. Schmid, and H. Coenen, PET quantitation and imaging of the non-pure positron-emitting iodine isotope ^{124}I, Applied Radiation and Isotopes, Vol.56, No. 5, pp. 673-679, 2002.

[3] Q. Bao, D. Newport, M. Chen, D. B. Stout, A. F. Chatziioannou, Performance evaluation of the inveon dedicated PET preclinical tomograph based on the NEMA NU-4 standards, Journal of Nuclear Medicine, Vol.50, No. 3, pp. 401-408, 2009.

[4] J. Mukherjee, and C. Constantinescu, Performance evaluation of an Inveon PET preclinical scanner, Physics in Medicine and Biology, Vol.54, No. 9, pp. 2885-2899, 2009.

[5] M. A. Bahri, A. Plenevaux, G. Warnock, A. Luxen, and A. Seret, NEMA NU4-2008 image quality performance report for the microPET focus 120 and for various transmission and reconstruction methods, Journal of Nuclear Medicine, Vol.50, No. 10, pp. 1730-1738, 2009.

[6] J. A. Disselhors, M. Brom, and P. Laverman, Image-quality assessment for several positron emitters using the NEMA NU 4-2008 standards in the Siemens Inveon small-animal PET scanner, Journal of Nuclear Medicine, Vol.51, No. 4, pp. 610-617, 2010.